

OH-Radical Induced Oxidation of Phenoxyacetic Acid and 2,4-Dichlorophenoxyacetic Acid. Primary Radical Steps and Products

Robert Zona,[†] Sonja Solar,^{*,†} Knud Sehested,[‡] Jerzy Holcman,[‡] and Stephen P. Mezyk[§]

Institute for Theoretical Chemistry and Structural Biology, University of Vienna, Althanstr. 14, A-1090 Vienna, Austria, Risoe National Laboratories, DK-4000 Roskilde, Denmark, and Department of Chemistry and Biochemistry, California State University, Long Beach, California 90840

Received: January 16, 2002; In Final Form: April 23, 2002

The reactions of $\bullet\text{OH}$ radicals with 2,4-dichlorophenoxyacetic acid (2,4-D), $k = (6.6 \pm 0.5) \times 10^9 \text{ M}^{-1} \text{ s}^{-1}$, phenoxyacetic acid (PAA), $k = (10 \pm 1) \times 10^9 \text{ M}^{-1} \text{ s}^{-1}$, and 2,4-dichlorophenol (2,4-DCP), $k = (7.1 \pm 0.5) \times 10^9 \text{ M}^{-1} \text{ s}^{-1}$, have been studied using pulse and gamma radiolysis. The $\bullet\text{OH}$ adducts produced by addition to the ring at positions not occupied by substituted groups were oxidized by $\text{K}_3[\text{Fe}(\text{CN})_6]$, with the corresponding hydroxylated species analyzed by HPLC. The distribution of $\bullet\text{OH}$ radical addition to the aromatic ring of 2,4-D is C1, 17%; C2/C4, 20%; C3/C5/C6, 47%; and for $\bullet\text{OH}$ reaction with PAA, it is C1, 5.5%; C2/C6, 45%; C3/C5, 11%; C4, 36%. Whereas the hydroxycyclohexadienyl radicals of 2,4-D have no observable reactivity toward oxygen, those of PAA and 2,4-DCP do react, with $k(\bullet\text{OH adduct-PAA}) + \text{O}_2 = (5.1 \pm 0.2) \times 10^8 \text{ M}^{-1} \text{ s}^{-1}$ and $k(\bullet\text{OH adduct-2,4-DCP}) + \text{O}_2 = (1.1 \pm 0.1) \times 10^8 \text{ M}^{-1} \text{ s}^{-1}$. The phenoxy radicals formed by chloride elimination from the ipso-chloro- $\bullet\text{OH}$ adducts of 2,4-D rapidly oxidize TMPD to $\text{TMPD}^{\bullet+}$, $k = (3.6 \pm 0.5) \times 10^9 \text{ M}^{-1} \text{ s}^{-1}$.

Introduction

The phenoxy acid herbicide 2,4-dichlorophenoxyacetic acid (2,4-D) is one of the most widely applied agrochemicals, and consequently, its presence as a contaminant and subsequent removal has been the focus of considerable study. Much effort has been put into investigations for its degradation by advanced oxidation processes (AOPs), which are based on in-situ oxidative destruction using $\bullet\text{OH}$ radicals. Photocatalytic and photo-Fenton treatments, as well as the combination of these methods with ozone, have been applied for 2,4-D removal.^{1–6} In some treatments, 2,4-dichlorophenol (2,4-DCP) was found as an intermediate product.^{1,4} The use of ionizing radiation for decomposition of 2,4-D in the presence of oxygen has been recently determined by our laboratory⁷ where with an absorbed dose of 4 kGy a total degradation of 500 μM 2,4-D and a 40% reduction of total organic carbon (TOC) was achieved.

The objective of the present study was to elucidate the primary patterns of $\bullet\text{OH}$ -radical attachment on 2,4-D and phenoxyacetic acid (PAA). The influence of the chlorine substituent on the $\bullet\text{OH}$ distribution on the aromatic ring and the effect of oxygen on the degradation rate of the hydroxycyclohexadienyl radicals of 2,4-D, PAA, and 2,4-DCP were determined.

Materials and Methods

Chemicals. The materials used were of the highest grade commercially available and were applied as received. 2,4-D, PAA, 2-methyl-4-chlorophenoxyacetic acid (MCPA), 2,4,5-trichlorophenoxyacetic acid (2,4,5-T), 2-methyl-4-chlorophenol (2-M-4-CP), and 2,4,5-trichlorophenol (2,4,5-TCP) were ob-

tained from Aldrich; 2,4-DCP, phenol, and $\text{K}_3[\text{Fe}(\text{CN})_6]$ were obtained from Merck, sodium chloride was obtained from Sigma, *N,N,N',N'*-tetramethyl-*p*-phenylenediamine (TMPD) was obtained from Fluka, N_2O (2.0) and O_2 (5.0) were obtained from Messer Griesheim Austria. All solutions were made immediately before irradiation, using Millipore filtered water containing less than 13 ppb TOC. For HPLC studies, Millipore filtered water and methanol (Promochem, HPLC-grade) were used for eluents.

Pulse Radiolysis Equipment. The 10 MeV LINAC at Risoe (Haimson Research Corp., HRC-712), providing pulses of 0.2–1 μs duration were used for most of these experiments.⁸ The detection system consisted of a 450 W xenon lamp, a quartz cell (light path: 5.1 cm), a Perkin-Elmer double quartz prism monochromator and a photomultiplier tube (IP28) connected to a model 9400 LeCroy digital oscilloscope, and an IBM PC/AT3 computer for on-line data processing. The absorbed dose was determined using a hexacyanoferrate(II)-dosimeter, with $G(\bullet\text{OH} + e_{\text{aq}}^-) = 6.6 \times 10^{-7} \text{ M J}^{-1}$, and $\epsilon_{420} = 1000 \text{ M}^{-1} \text{ cm}^{-1}$.⁹ The measured transient absorptions were normalized to a dose of 10 Gy and OD/cm. Some data were also measured using the LINAC system at the Radiation Laboratory, University of Notre Dame.¹⁰ Dosimetry for this system was performed using N_2O -saturated 10^{-2} M KSCN solutions at $\lambda = 475 \text{ nm}$ ($G\epsilon = 5.2 \times 10^{-4} \text{ m}^2 \text{ J}^{-1}$)¹¹ with average doses of 4–5 Gy per 3 ns pulse. All of these measurements were performed at ambient temperature ($22 \pm 2^\circ \text{C}$). The uncertainty of the kinetic data obtained by these pulse radiolysis measurements is estimated as ± 5 –10%.

γ Irradiations. γ irradiations were carried out in a ^{60}Co - γ -source (“Gammacell 220”, Nordion International Inc., Kanata, Ontario, Canada) with dose rates of 75–80 Gy min^{-1} , as determined by Fricke dosimetry, $G(\text{Fe}^{3+}) = 16.16 \times 10^{-7} \text{ M J}^{-1}$.¹²

Analysis. Substrate degradation and product formation after irradiation were determined by HPLC (Hewlett-Packard series

* To whom correspondence should be addressed. Phone: +43-1-4277-52725. Fax: +43-1-4277-52795. E-mail: sonja.solar@univie.ac.at.

[†] University of Vienna.

[‡] Risoe National Laboratories.

[§] California State University.

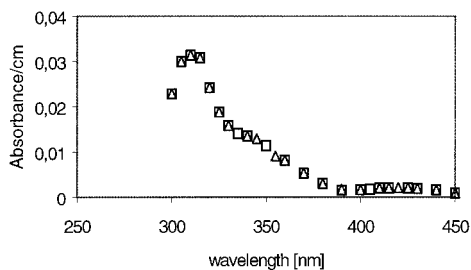


Figure 1. UV absorption spectra resulting from the reaction of OH radicals with 2,4-D (500 μ M) in N_2O (open triangle) and N_2O/O_2 (open square) saturated solutions (pH 9.1). 2–4 μ s after pulse; normalized to 10 Gy.

1050 and 1100, Hypersil ODS 2 RP-18 (5 μ m) column; flow rate: 1 mL/min, eluent: $H_2O(0.1\% H_3PO_4)/CH_3OH = 55:45$ per volume). The decomposition of the phenoxyacetic acids and the formation of product phenol, 2-M-4-CP, 2,4-DCP, and 2,4,5-TCP, was followed by a multiple wavelength UV detector with diode array at 210 nm.

The hydroxylated products of PAA and 2,4-D were quantified by electrochemical detection (amperometric detection: glassy carbon working electrode, Ag/AgCl reference electrode and carbon auxiliary electrode; oxidation mode: + 0.9 V).

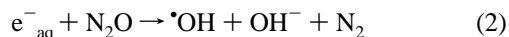
Quantitative analysis of product chloride was carried out by HPLC, using an indirect absorption technique via phthalations (column: ashipak ODP-50, flow rate: 1.5 mL/min, eluent: $H_2O/CH_3CN/Hewlett-Packard$ mobile phase, ratio 81/14/5, pH 8.6, according to the manufacturers instructions).

Results and Discussion

Pulse Radiolysis. N_2O Saturated Solutions. Electron pulse radiolysis experiments were performed in order to obtain the spectroscopic and kinetic characteristics of the intermediates from the reactions of $\bullet OH$ radicals with 2,4-D, PAA, and 2,4-DCP. The radiolysis of water leads to the formation of $\bullet OH$ radicals, solvated electrons, e^-_{aq} , and H atoms:



The radiation chemical yields (G values) of these primary radicals are $G(\bullet OH) \cong G(e^-_{aq}) \cong 2.9 \times 10^{-7} M J^{-1}$ and $G(H\bullet) = 0.6 \times 10^{-7} M J^{-1}$. Solvated electrons with N_2O producing further $\bullet OH$ radicals, reaction 2:



with $k_2 = 9.1 \times 10^9 M^{-1} s^{-1}$.¹³ Thus, in the pH range 4–10, the yield of hydroxyl radicals is $G(\bullet OH) = 5.8 \times 10^{-7} M J^{-1}$.

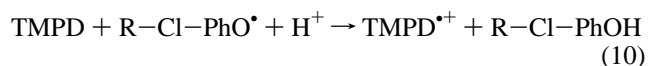
The UV-absorption spectrum resulting from the $\bullet OH$ adducts (including that of $\sim 10\%$ $\bullet H$ atoms) of 2,4-D in N_2O saturated solution is presented in Figure 1.

Hydroxyl radicals react mainly by addition to the ring, giving rise to hydroxycyclohexadienyl radicals. Such radicals typically have absorption maxima at ~ 310 nm. In the case of 2,4-D, the $\bullet OH$ adducts (Scheme 1) absorb between 300 and 370 nm with $\lambda_{max} = 310\text{--}315$ nm and $\epsilon_{max} = 5600 M^{-1} cm^{-1}$ (corrected for $\bullet H$ -atom contribution). The calculation of this molar absorbance ϵ for the $\bullet OH$ adducts assumed that the reaction of the $\bullet OH$ radicals with 2,4-D was quantitative and that all of the $\bullet OH$ adducts have the same molar absorbance at the peak wavelength. The absorptions from 390 to 450 nm are characteristic for phenoxy radicals, produced by reactions 5 and 7. Ipso-chloro- $\bullet OH$ adducts are known to eliminate HCl spontaneously.¹⁴ The transients formed, by $H\bullet$ abstraction from the acetic acid group,

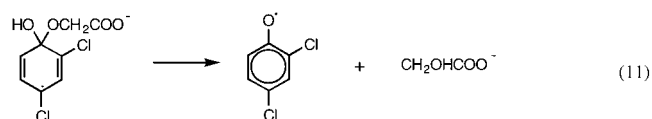
(reaction 3, Scheme 1) are expected to absorb below 300 nm (cf. 4-chlorobenzyl radicals which have an absorption maximum at 268 nm)¹⁵ and cannot be optically detected because of the strong absorption of the substrate in this wavelength range.

The kinetics of the $\bullet OH$ radical reactions was examined by following the absorption growth at λ_{max} of the $\bullet OH$ adducts. This was done at different 2,4-D concentrations ($4\text{--}10 \times 10^{-5} M$), with the overall second-order rate constant of the oxidation process determined from plots of the pseudo-first-order growth rates versus 2,4-D concentration. The rate constant for the overall reaction of $\bullet OH$ with 2,4-D was determined to be $k(\bullet OH + 2,4-D) = (6.6 \pm 0.5) \times 10^9 M^{-1} s^{-1}$.

To obtain the initial yield of the chlorophenoxy radicals ($R-Cl-PhO\bullet$, $R = -OCH_2COO^-$) (reactions 5 and 7, Scheme 1), they were reduced by TMPD, giving the $TMPD^{\bullet+}$ radical cation which has an absorption maximum at $\lambda = 565$ nm ($\epsilon_{max} = 12500 M^{-1} cm^{-1}$).¹⁶ From the growth profile of the $TMPD^{\bullet+}$ absorption at 565 nm (Figure 2), a rate constant for the electron transfer, $k_{10}(TMPD + R-Cl-PhO\bullet) = (3.6 \pm 0.2) \times 10^9 M^{-1} s^{-1}$, was obtained:



One of the main radiolytic products of 2,4-D is 2,4-DCP (see gamma radiolysis results, Table 3). Its formation can be assumed to occur via an $\bullet OH$ -addition/glycolic acid elimination step, reaction 11, by analogy to the demethoxylation process of methoxylated benzoic acids and benzenes.^{17,18}



To determine whether the ipso- $\bullet OH$ -adducts on position 1 of 2,4-D can rapidly form phenoxy radicals, investigations on other phenoxyacetic acids (PAA, MCPA, and 2,4,5-T) have been carried out. The yields of $TMPD^{\bullet+}$ radical cations are compiled in Table 1. The G values as well as k_{10} represent mean values obtained from phenoxyacetic acids solutions (230 μ M) with three different TMPD concentrations: 10, 20, and 40 μ M. The yields of product phenols, formally arising from substitution of $-OCH_2COO^-$ by $-OH$, have been determined after gamma-radiolysis in N_2O and are given for comparison.

Whereas the fraction of phenol formed for all investigated phenoxyacetic acids is very similar (15–20% of $\bullet OH$), the production of $TMPD^{\bullet+}$ is strongly dependent on the number of chlorine atoms. For the chlorine free compound PAA, it is practically negligible (3.6% of $\bullet OH$). Chlorine in the molecule causes an increase of $\sim 10\%$ $TMPD^{\bullet+}$ absorption per Cl atom. Accordingly, it can be concluded that only those radicals resulting from HCl elimination of the phenoxyacetic acid $\bullet OH$ adducts are oxidizing species. They reflect the amount of $\bullet OH$ radicals, added to ring positions carrying the halogen group. Because the ipso- $\bullet OH$ -adducts formed on position 1 of the phenoxyacetic acids do not contribute to TMPD oxidation, the formation of phenoxy radicals via reaction 11 can be assumed as slow compared to HCl elimination, reactions 5 and 7.

The $\bullet OH$ adduct spectrum of PAA is shown in Figure 3. It exhibits a strong absorption band between 320 and 330 nm, with a calculated $\epsilon_{325} = 5400 M^{-1} cm^{-1}$. The absorption above 400 nm is negligible. The rate constant for the overall reaction

SCHEME 1: Reactions 3–9

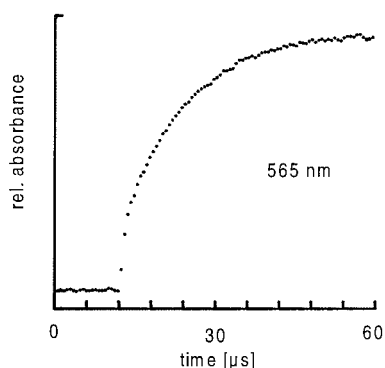
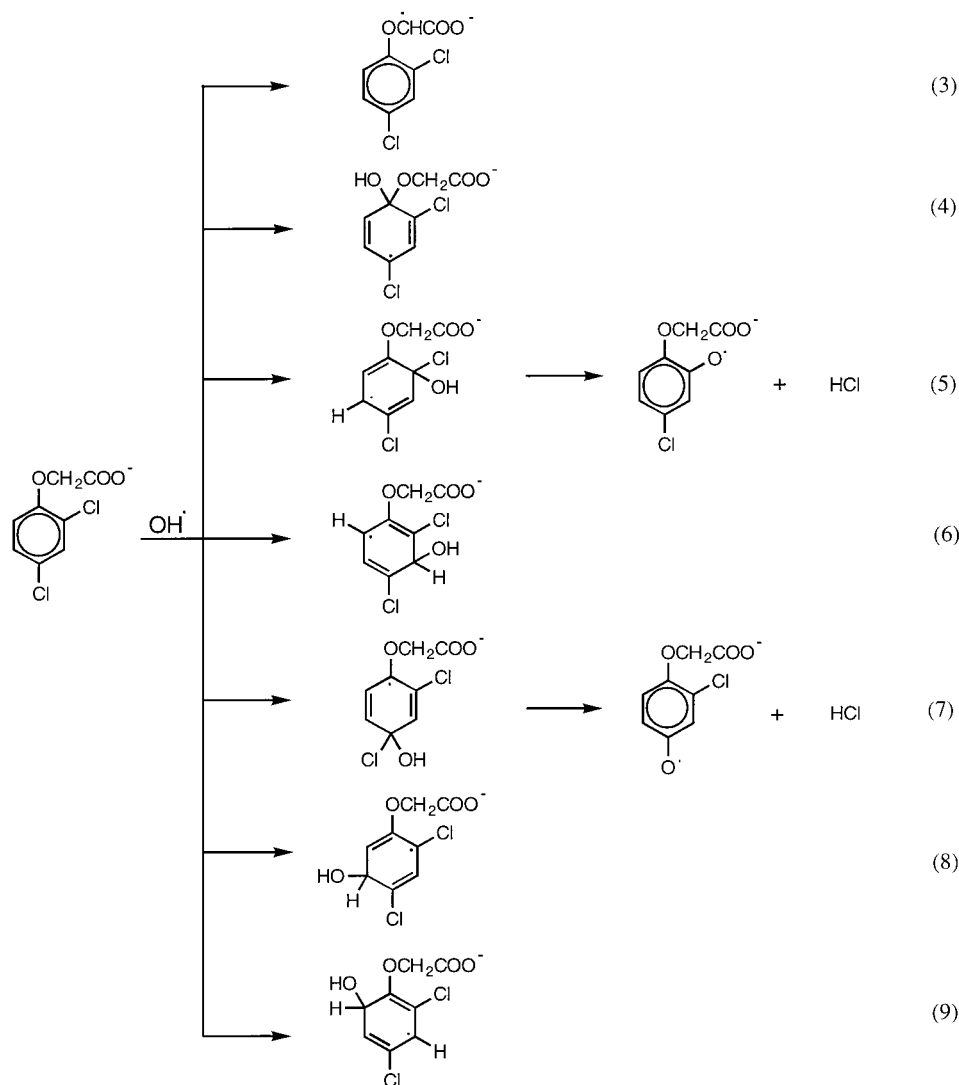


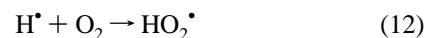
Figure 2. Pulse radiolysis (8 Gy/pulse, pulse length 0.4 μs) of N_2O saturated aqueous solution of 2,4-D (2.3×10^{-4} M) containing TMPD (2×10^{-5} M) at pH 10. Formation of the $\text{TMPD}^{\bullet+}$ measured by its absorption at 565 nm as a function of time.

of $\bullet\text{OH}$ with PAA was determined from the concentration dependence of the growth of the absorptions at 315 and 320 nm giving $k(\bullet\text{OH} + \text{PAA}) = (10 \pm 1.0) \times 10^9 \text{ M}^{-1} \text{ s}^{-1}$.

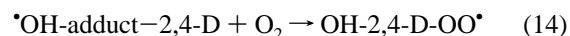
The transient absorption spectrum resulting from the $\bullet\text{OH}$ -adduct formation with 2,4-DCP is presented in Figure 4. The main absorption band is centered at 310 nm, $\epsilon_{\text{max}} = 6900 \text{ M}^{-1} \text{ cm}^{-1}$. The phenoxyl radical absorption is comparable to that of 2,4-D. A rate constant $k(\bullet\text{OH} + 2,4\text{-DCP}) = (7.1 \pm 0.5) \times 10^9$

$\text{M}^{-1} \text{ s}^{-1}$ was obtained from the growth of absorption at 310 nm.

Presence of Oxygen. In the presence of air (oxygen concentration 0.25 mM), H atoms and e_{aq}^- are transformed into $\text{HO}_2^\bullet/\text{O}_2^{\bullet-}$, depending on the pH of the solution, (reactions 12 and 13, $k_{12} = 2.1 \times 10^{10} \text{ M}^{-1} \text{ s}^{-1}$, $k_{13} = 1.9 \times 10^{10} \text{ M}^{-1} \text{ s}^{-1}$, $\text{p}K(\text{HO}_2^\bullet) = 4.8$:¹³



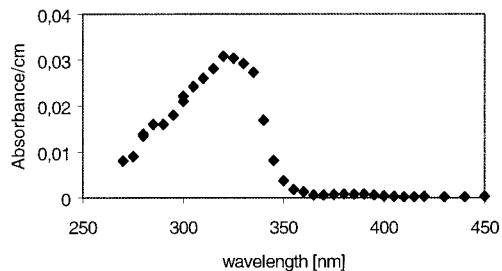
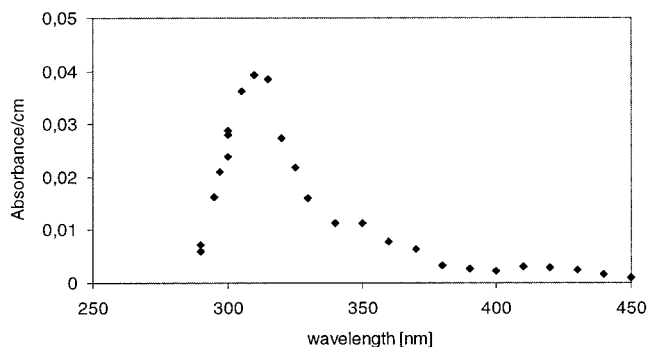
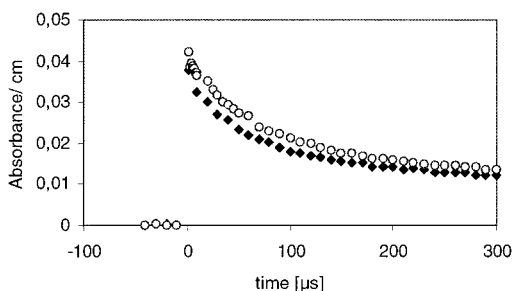
In solutions saturated with $\text{N}_2\text{O}/\text{O}_2$ (4:1 v/v), addition of oxygen to the radicals derived from $\bullet\text{OH}$ reaction with 2,4-D to form hydroxycyclohexadienylperoxyl radicals is expected (reaction 14):



The transient absorption spectrum obtained under $\text{N}_2\text{O}/\text{O}_2$ conditions is presented in Figure 1. The spectrum in $\text{N}_2\text{O}/\text{O}_2$ is practically identical to that in only N_2O , indicating that the presence of oxygen does not influence the yield of the $\bullet\text{OH}$ adducts. To determine the rate constant $k_{14}(\bullet\text{OH-adducts-2,4-D} + \text{O}_2)$, an appropriate pressure cell to obtain high oxygen

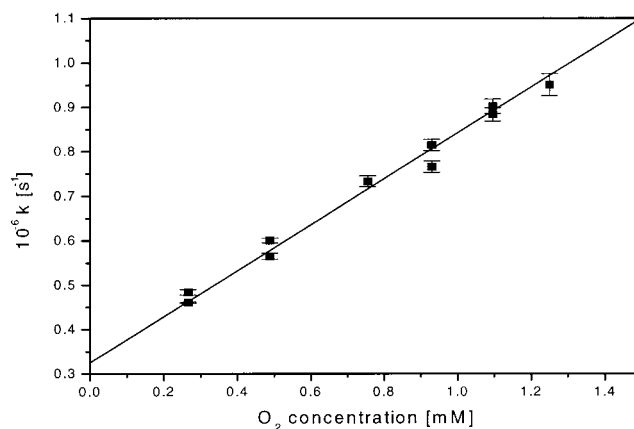
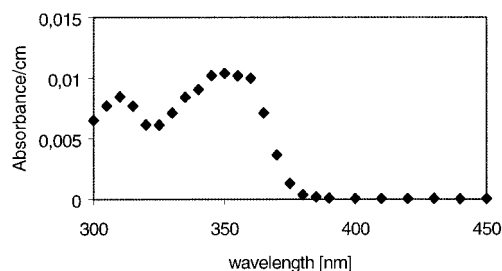
TABLE 1: G Values of $\text{TMPD}^{\bullet+}$ Radical Cations (Pulse Radiolysis) and Yields of Phenols (Initial G Values, Determined after Gamma Radiolysis) as Well as Their Yields Relative to $G(\bullet\text{OH})$ for Various Phenoxyacetic Acids ($500 \mu\text{M}$) in N_2O Saturated Solution, pH 9.2–9.4

phenoxyacetic acids	$G(\text{TMPD}^{\bullet+})$ $\times 10^{-7} \text{MJ}^{-1}$	% relative to $G(\bullet\text{OH})$	phenols	$G_i(\text{phenols})$ $\times 10^{-7} \text{MJ}^{-1}$	% relative to $G(\bullet\text{OH})$
PAA	0.21 ± 0.02	3.6	phenol	0.83 ± 0.08	14.5
MCPA	0.73 ± 0.05	12.7	2-M-4-CP	1.14 ± 0.1	20
2,4-D	1.24 ± 0.1	21.8	2,4-DCP	1.08 ± 0.1	19
2,4,5-T	1.61 ± 0.1	28.2	2,4,5-TCP	1.0 ± 0.1	17.6

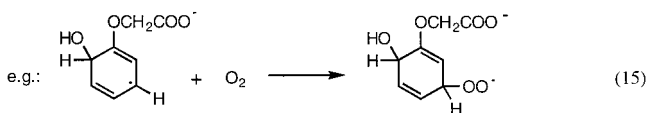
**Figure 3.** UV absorption spectrum resulting from the reaction of OH radicals with PAA ($500 \mu\text{M}$) in N_2O saturated solutions (pH 9.1). 2–4 μs after pulse; normalized to 10 Gy.**Figure 4.** UV absorption spectrum resulting from the reaction of OH radicals with 2,4-DCP ($500 \mu\text{M}$) in N_2O saturated solutions (pH 5.9). 2–4 μs after pulse; normalized to 10 Gy.**Figure 5.** Absorption at 320 nm as a function of time [μs] obtained in N_2O (circle) and $\text{N}_2\text{O}/\text{O}_2$ (diamond: 490 mM $\text{N}_2\text{O}/25 \text{ mM O}_2$) saturated solutions, $500 \mu\text{M}$ 2,4-D, pH 9.1, dose: 10.1 Gy

concentrations was used.¹⁹ The ratios of $\text{O}_2/\text{N}_2\text{O}$ were varied from 5 to 30 bar $\text{O}_2/25$ –45 bar N_2O , corresponding to ratios of 6.25–37.5 mM $\text{O}_2/490$ –890 mM N_2O . The absorptions at 320 nm did not show any significant change as a function of oxygen concentration in the time scale observable by pulse radiolysis (ms). Oscilloscope traces for N_2O and $\text{N}_2\text{O}/\text{O}_2$ saturated solutions are presented in Figure 5.

This result is consistent with earlier gamma-radiolysis investigations in the presence of oxygen, where no dependence of the initial degradation rates of 2,4-D on oxygen concentration was observed.⁷ Although the rate constant of the hydroxycyclohexadienyl radicals with O_2 is too slow to be measured here, there is a strong indication that these radicals do react with oxygen. In recent investigations, a high oxygen uptake had been

**Figure 6.** Rate constant determination for reaction of PAA–OH adduct with O_2 in aqueous solution. Weighted linear fit gives rate constant of $(5.13 \pm 0.20) \times 10^8 \text{ M}^{-1} \text{ s}^{-1}$.**Figure 7.** UV absorption spectrum resulting from the reaction of H radicals with 2,4-D ($500 \mu\text{M}$) in Ar saturated solutions (pH 1.2, 0.5 M *t*-BuOH). 10 μs after pulse; normalized to 10 Gy.

reported, at 1 kGy its yield was $G(\text{O}_2 \text{ uptake}) = 2.38 \times 10^{-7} \text{ M J}^{-1}$.⁷ This may be attributed to fast reactions of the radiolytic products. For the $\bullet\text{OH}$ adducts of 2,4-DCP, a major product of 2,4-D radiolysis, the subsequent reaction with oxygen was $k(\bullet\text{OH-adducts} + 2,4\text{-DCP} + \text{O}_2) = (1.1 \pm 0.1) \times 10^8 \text{ M}^{-1} \text{ s}^{-1}$. For the $\bullet\text{OH}$ adducts of PAA, which has no chlorine substituent, an even higher reactivity was found, with $k_{15}(\bullet\text{OH-adducts} + \text{PAA} + \text{O}_2) = (5.1 \pm 0.2) \times 10^8 \text{ M}^{-1} \text{ s}^{-1}$ (Figure 6). These rate constants are consistent with previous literature reports that hydroxycyclohexadienyl radicals with electron withdrawing substituents have less reactivity toward oxygen.^{20,21}



Reactions with H^\bullet and e^-_{aq} . The transients resulting from the reaction of H^\bullet atoms with 2,4-D have been studied at pH 1.2 ($\text{H}^+ + e^-_{\text{aq}} \rightarrow \text{H}^\bullet$, $k = 2.2 \times 10^{10} \text{ M}^{-1} \text{ s}^{-1}$ ¹³) in the presence of 0.5 M *tert*-butyl alcohol as $\bullet\text{OH}$ scavenger, $k(\bullet\text{OH} + \text{tert-butyl alcohol}) = 5.5 \times 10^8 \text{ M}^{-1} \text{ s}^{-1}$.¹³ Under these experimental conditions, $G(\text{H}^\bullet) = 3.7 \times 10^{-7} \text{ M J}^{-1}$. The transient absorption spectrum, Figure 7, has a broad maximum at $\lambda_{\text{max}} = 350 \text{ nm}$ with $\epsilon_{\text{max}} = 3600 \text{ M}^{-1} \text{ cm}^{-1}$ and represents all of the H^\bullet adducts

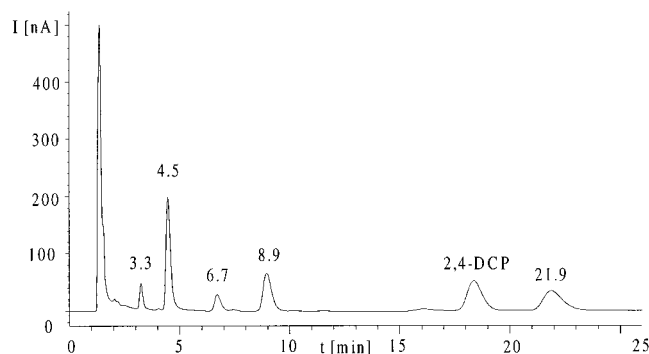
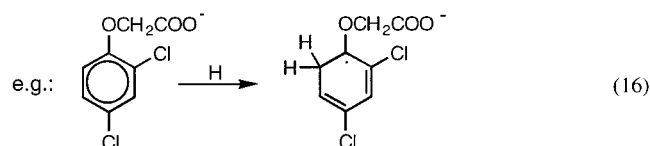


Figure 8. HPLC chromatogram: ECD (+0.9 V), 5×10^{-4} M 2,4-D, 5×10^{-4} M $K_3Fe(CN)_6$, pH 9, N_2O saturated, dose: 100 Gy; retention time (Rt) 3.3 and 6.7 min, $C_8H_7ClO_4$; Rt 4.5, 8.9, and 21.9 min, $C_8H_6Cl_2O_4$.

TABLE 2: Compilation of the Kinetic Data Obtained by Pulse Radiolysis in This Study

reaction	rate constants, $M^{-1} s^{-1}$
$e^-_{aq} + 2,4-D$	$(2.5 \pm 0.3) \times 10^9$
$H^+ + 2,4-D$	$(1.4 \pm 0.1) \times 10^9$
$\cdot OH + 2,4-D$	$(6.6 \pm 0.5) \times 10^9$
$\cdot OH + PAA$	$(10 \pm 1.0) \times 10^9$
$\cdot OH + 2,4-DCP$	$(7.1 \pm 0.5) \times 10^9$
$TMPD + R-Cl-PhO\cdot$	$(3.6 \pm 0.2) \times 10^9$
$\cdot OH\text{-adduct-}2,4-D + O_2$	not observable
$\cdot OH\text{-adduct-}2,4-D + K_3[Fe(CN)_6]$	$< 5 \times 10^5$
$\cdot OH\text{-adduct-PAA} + O_2$	$(5.1 \pm 0.2) \times 10^8$
$\cdot OH\text{-adduct-}2,4-DCP + O_2$	$(1.1 \pm 0.1) \times 10^8$

formed (e.g., via reaction 16). From the absorbance change at 350 nm, an overall rate constant of $k_{16}(H^+ + 2,4-D) = (1.4 \pm 0.1) \times 10^9 M^{-1} s^{-1}$ was obtained.



The reaction of e^-_{aq} with 2,4-D was determined from the first-order rates of absorbance loss for e^-_{aq} at 600 nm, $k(e^-_{aq} + 2,4-D) = (2.5 \pm 0.3) \times 10^9 M^{-1} s^{-1}$ (solution: 200–500 μM 2,4 D, pH 9, 0.5 M *tert*-butyl alcohol, Ar).

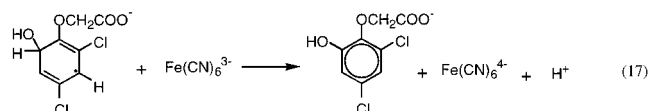
TABLE 3: Initial G Values ($10^{-7} M J^{-1}$) for Products Formed under the Different Oxidizing Conditions for Radiolysis of 2,4-D (500 μM , pH 9) as Well as Their Corresponding Yields Relative to $\cdot OH$ -Radical Concentration

products	N_2O		N_2O/O_2		$N_2O/K_3[Fe(CN)_6]$	
	G_i	% ($\cdot OH$)	G_i	% ($\cdot OH$)	G_i	% ($\cdot OH$)
2,4-diCl-OH-PAA 4.5 min	0.21	3.6	0.04	0.7	1.14	20
2,4-diCl-OH-PAA 8.9 min	0.10	1.8	0.07	1.3	0.67	12
2,4-diCl-OH-PAA 21.9 min	0.13	2.4	0.03	0.5	0.85	15
OH-Cl-PAA, 3.3 min	0.09	1.6	0.17	2.9	0.17	2.9
OH-Cl-PAA, 6.7 min	0.18	3.1	0.18	3.1	0.18	3.1
2,4-DCP	1.08	19	1.08	19	0.98	17
Phenolic products total	1.79	32	1.59	28	4	70

TABLE 4: Initial G Values ($10^{-7} M J^{-1}$) for Products Formed under the Different Oxidizing Conditions for Radiolysis of PAA (500 μM , pH 9) as Well as Their Corresponding Yields Relative to $\cdot OH$ -Radical Concentration

products	N_2O		N_2O/O_2		$N_2O/K_3[Fe(CN)_6]$	
	G_i	% ($\cdot OH$)	G_i	% ($\cdot OH$)	G_i	% ($\cdot OH$)
OH-PAA 11.1 min (ortho)	0.31	5.5	1.30	22.7	2.59	45
OH-PAA 7.6 min (meta)	0.10	1.8	0.10	1.8	0.62	11
OH-PAA 5.5 min (para)	0.31	5.5	0.49	8.5	2.07	36
Phenol	0.83	14.5	0.41	7.3	0.31	5.5
Phenolic products total	1.55	27.3	2.3	40.3	5.59	97.5

Gamma Radiolysis. To obtain further information on the distribution of $\cdot OH$ reaction at the various positions of 2,4-D in comparison with PAA, gamma irradiations in the presence of $N_2O/K_3[Fe(CN)_6]$ were performed. With $Fe(CN)_6^{3-}$ (redox potential $E^\circ = 360 mV^{22}$), the nonipso- $\cdot OH$ adducts of benzene derivatives are oxidized to the corresponding phenols.^{20,22,23} Even for benzonitrile, which has the strongly electron withdrawing $-CN$ group, a quantitative oxidation of its hydroxycyclohexadienyl radicals to *o*-, *m*-, and *p*-hydroxybenzonitrile could be achieved.²¹ The electron-transfer reaction for 2,4-D is demonstrated on the C6- $\cdot OH$ -adduct, reaction 17:



A rate constant for this oxidation process of $k_{17} < 5 \times 10^5 M^{-1} s^{-1}$ was obtained from pulse radiolysis measurements. This value is consistent to that of the oxidation of the hydroxycyclohexadienyl radicals of benzonitrile, where $k = < 2 \times 10^5 M^{-1} s^{-1}$.²⁰

The phenolic products formed upon gamma radiolysis of 2,4-D in the presence of $N_2O/K_3[Fe(CN)_6]$ are presented in the HPLC chromatogram, Figure 8.

In addition to 2,4-DCP, five products are generated when 2,4-D is irradiated under these conditions. These products were identified from the mass spectra obtained by HPLC/ESI-MS analysis, (M-1) mode.⁷ The compounds with retention times (Rt.) 4.5, 8.9, and 21.9 min have two chlorine atoms and could be qualified as the isomers of the hydroxylation products, *m/z* 235. A precise correlation to 3-, 5-, and 6-hydroxy-2,4-dichloroacetic acids (2,4-diCl-OH-PAA) cannot be given. The products at Rt. 3.3 and 6.7 min result from the monochloro-derivatives of 2,4-D (2-chloro-4-hydroxy- and 4-chloro-2-hydroxyphenoxyacetic acid, OH-Cl-PAA, *m/z* 200.6), having the ipso-chloro- $\cdot OH$ adducts, and consequently the corresponding phenoxyl radicals, as precursors. Because of the lack of calibration standards for these compounds, their quantification by HPLC could only be estimated. The evaluation was done by amperometric detection, +0.9 V. This particular detection system was used because the amperometric signal intensity dependence upon compound concentration was very similar for all chlorophenols studied. The slopes of the calibration curves

for the following compounds are all within 10%: phenol ($y = 282x$, $R^2 = 0.998$), 2-chlorophenol ($y = 283x$, $R^2 = 0.999$), 3-chlorophenol ($y = 315x$, $R^2 = 0.997$), 4-chlorophenol ($y = 287x$, $R^2 = 0.996$), and 2,4-dichlorophenol ($y = 258x$, $R^2 = 0.999$). Therefore, a mean value of these data, $y = 285x$, was taken for the quantification of the hydroxylated derivatives of 2,4-D. Similar experiments and analysis were also carried out for PAA measurements.

The G values, obtained from the linear part of the yield vs dose plots for the radiolytic products of 2,4-D and PAA under various oxidation conditions, are summarized in Tables 3 and 4.

For PAA in the presence of $K_3[Fe(CN)_6]$, a quantitative material balance could be achieved. The fractions of $\cdot OH$ -adduct distribution on the ring positions ipso:ortho:meta:para was 0.06:0.45:0.11:0.36. Attack on the side chain obviously plays a minor role. These results are comparable to that reported for anisole, ipso:ortho:meta:para = 0.07:0.48:0.07:0.38.²²

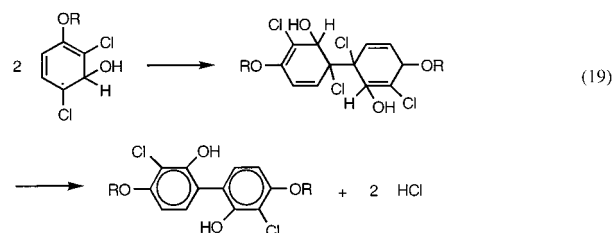
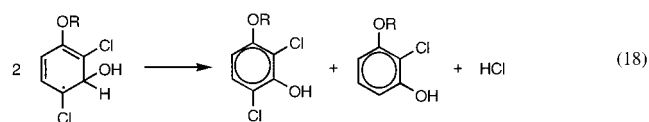
The presence of two chlorine atoms on the phenoxyacetic acid molecule changes the pattern of $\cdot OH$ addition into a more statistical distribution. For 2,4-D, the total yield of hydroxylation on C6, C3, and C5 (2,4-diCl-OH-PAA), detected by oxidation with $K_3[Fe(CN)_6]$, is 47%. Because the product at 4.5 min (Figure 8, Table 3) is formed with the highest yield, 20% of the initially generated $\cdot OH$ radicals, it can be assumed to be 2,4-dichloro-6-hydroxyphenoxyacetic acid, arising from the $\cdot OH$ adduct on the free ortho position of the molecule, reaction 9, Scheme 1. The products resulting from the meta adducts, 3- and 5-hydroxy-2,4-dichlorophenoxyacetic acid, contribute 27% of the total reaction. Because of the ortho-para directing chlorine substituents, the $\cdot OH$ attachment on the meta positions of 2,4-D is significantly higher than for PAA, where only 11% of 3- and 5-hydroxyphenoxyacetic acid were produced. The yield of 2,4-DCP (17%) corresponds to the fraction of the $\cdot OH$ attack on C1.

Because phenoxy radicals, which are precursors of 2-chloro-4-hydroxy- and 4-chloro-2-hydroxyphenoxyacetic acid (OH-Cl-PAA), are not oxidized by $K_3[Fe(CN)_6]$, the yield of 6% (Table 3) does not reflect the primary $\cdot OH$ attack. This has to be determined from the TMPD experiments, where about 20% of the phenoxy radicals could be detected (Table 1). Summarizing the data from both series, as fractions of $\cdot OH$ reaction with 2,4-D, gives C1, 0.17; C2/C4, 0.20; C3/C5, 0.27; and C6, 0.20, demonstrating little preference for any of the positions on the ring. The material balance is 84% of the total $\cdot OH$ reaction. From this result, one could conclude that 16% of hydroxyl radicals react with the side chain, however, this appears relatively high compared to PAA, where this process contributed only <3%. However, the low value of $k_{17} < 5 \times 10^5 \text{ M}^{-1} \text{ s}^{-1}$ also means that bimolecular decay of the OH adducts will also occur in competition to the $K_3[Fe(CN)_6]$ oxidation process which would readily account for the lower material balance observed.

In N_2O/O_2 (4:1 v/v) saturated solutions, the total formation of phenolic products from 2,4-D is very similar to that in the presence of N_2O , 28% and 32% (Table 3). This confirms the pulse radiolysis results, showing that the hydroxycyclohexadienyl radicals of 2,4-D have a very low reactivity toward oxygen. For PAA, where a reaction of oxygen by the $\cdot OH$ adducts was observable ($k_{15} = (5.1 \pm 0.2) \times 10^8 \text{ M}^{-1} \text{ s}^{-1}$), a considerable increase of 2-hydroxyphenoxyacetic acid from 5.5% in N_2O to 22.7% in N_2O/O_2 (Table 4) occurred.

For 2,4-D, product chloride determination after gamma radiolysis in N_2O has also been performed to correlate its production to that of chlorophenoxy radical generation (R-

Cl-PhO \cdot), measured by TMPD \cdot^+ formation (reaction 10) via pulse radiolysis, Table 1. The chloride yields after steady-state radiolysis, however, gave an initial concentration of $G(Cl^-) = 2.07$, corresponding to 33% of $\cdot OH$ which is much higher than the phenoxy radical concentration. This indicates that the product chloride results from both the first-order decay of the ipso-chloro- $\cdot OH$ adducts, reactions 5 and 7, Scheme 1, and also from second-order reactions of other chloro-hydroxycyclohexadienyl radicals. The meta $\cdot OH$ -adducts (reaction 6 and 8) may undergo disproportionation with a chloride release reaction 18 or combination at the chlorine substituted carbons. Such dimers are expected to eliminate HCl very efficiently, e.g., reaction 19 ($R = -CH_2COO^-$). An HX ($X = F, Cl$) release from a product of similar disproportionations and/or dimerizations has been observed by pulse radiolysis with conductivity measurements for the $\cdot OH$ adducts of fluoro- and chlorobenzene.²⁰



Summary

Electron pulse radiolysis and gamma radiolysis experiments, together with product analysis by HPLC, have been performed to elucidate the primary patterns of $\cdot OH$ radical attack on phenoxyacetic acid (PAA) and 2,4-dichlorophenoxyacetic acid (2,4-D). In the gamma radiolysis experiments, the yield of primary $\cdot OH$ adducts on positions not occupied by chlorine atoms were determined by oxidation with $K_3[Fe(CN)_6]$ to the corresponding hydroxylated compounds. The ipso-chloro- $\cdot OH$ adducts have been quantified via their phenoxy radicals, formed in a spontaneous HCl elimination step. These rapidly oxidize TMPD to TMPD \cdot^+ , as measured by pulse radiolysis. For PAA, the $\cdot OH$ attachment preferentially takes place on ortho and para positions to the acetic acid group, whereas for the dichlorinated compound 2,4-D, a more statistically distribution of $\cdot OH$ addition to the molecule takes place. In contrast to PAA, the $\cdot OH$ adducts of 2,4-D showed no significant reaction with oxygen.

Acknowledgment. The use of the equipment of the RISOE National Laboratory is gratefully acknowledged. S.P.M. acknowledges the time and help of the personnel at the Radiation Laboratory, University of Notre Dame, which is supported by the Office of Basic Energy Sciences of the U.S. Department of Energy. R.Z. thanks the University of Vienna for a stipend for his stay in Denmark.

References and Notes

- (1) Sun, Y.; Pignatello, J. J. *Environ. Sci. Technol.* **1993**, *27*, 304.
- (2) Sun, Y.; Pignatello, J. J. *Environ. Sci. Technol.* **1995**, *29*, 2065.
- (3) Modestov, A. D.; Lev, O. J. *Photochem. Photobiol. A: Chem.* **1998**, *112*, 261.

- (4) Herrmann, J. M.; Disdier, J.; Pichat, P.; Malato, S.; Blanco, J. *Appl. Catal. B: Environ.* **1998**, 17, 15.
- (5) Müller, T. S.; Sun, Z.; Kumar, G.; Itoh, K.; Murabayashi, M. *Chemosphere* **1998**, 36, 2043.
- (6) Piera, E.; Calpe, J. C.; Brillas, E.; Domenech, X.; Peral, J. *Appl. Catal. B: Environ.* **2000**, 27, 169.
- (7) Zona, R.; Solar, S.; Gehringer, P. *Wat. Res.* **2002**, 36, 1369.
- (8) Sehested, K.; Corfitzen, H.; Christensen, H. C.; Hart, E. J. *J. Phys. Chem.* **1975**, 79, 310.
- (9) Schuler, R. H.; Hartzell, A. L.; Behar, B. *J. Phys. Chem.* **1981**, 85, 192.
- (10) Whitman, K.; Lyons, S.; Miller, R.; Nett, D.; Treas, P.; Zante, A.; Fessenden, R. W.; Thomas, M. D.; Wang, Y. *Proceedings of the 95 Particle Accelerator Conference and International Conference on High Energy Accelerators*, 1996.
- (11) Buxton, G. V.; Stuart, C. R. *J. Chem. Soc., Faraday Trans.* **1995**, 91, 279.
- (12) Fricke, H.; Hart, E. J., Eds.; *Radiation Dosimetry*; Academic Press: New York, 1966.
- (13) Buxton, G. V.; Greenstock, C. L.; Helman, W. P.; Ross, A. B. *J. Phys. Chem. Ref. Data* **1988**, 17.
- (14) Latif, N.; O'Neill, P.; Schulte-Frohlinde, D.; Steenken, S. *Ber. Bunsen-Ges. Phys. Chem.* **1978**, 82, 468.
- (15) Merga, G.; Schuchmann, H.-P.; Madhava, Rao B. S.; von Sonntag, C. *J. Chem. Soc., Perkin Trans. 2* **1996**, 551.
- (16) Fujita, S.; Steenken, S. *J. Am. Chem. Soc.* **1981**, 103, 2540.
- (17) O'Neill, P.; Schulte-Frohlinde, D.; Steenken, S. *J. Chem. Soc., Faraday Discuss.* **1977**, 63, 141.
- (18) Gaisberger, B.; Solar, S. *Can. J. Chem.* **2001**, 79, 394.
- (19) Christensen, H. C.; Sehested, K. *Radiat. Phys. Chem.* **1980**, 16, 183.
- (20) Buxton, G. V.; Langan, J. R.; Smith, J. R. L. *J. Phys. Chem.* **1986**, 90, 0, 6309.
- (21) Fang, X.; Pan, X.; Rahmann, A.; Schuchmann, H. P.; von Sonntag, C. *Chem. Eur. J.* **1995**, 1, 423.
- (22) Raghavan, N. V.; Steenken, S. *J. Am. Chem. Soc.* **1980**, 102, 3495.
- (23) Steenken, S.; Raghavan, N. V. *J. Phys. Chem.* **1979**, 83, 3101.